fluorosulfate, $CH_3CH_2OSO_2F$, in about 45% yield. (*Caution!* Trap-to-trap distillation should be carried out carefully. Explosions occurred when the liquid-nitrogen Dewar was removed from the trap.) The ^{19}F NMR spectrum of $CH_3CH_2OSO_2F$ is comprised of a multiplet at ϕ +36.7 assigned to S-F. The ^1H NMR spectrum shows resonances at δ 1.5 (doublet of triplets, $^3J_{HH}$ = 7.3 Hz, $^5J_{HF}$ < 0.5 Hz) assigned to $-CH_3$ and at δ 4.6 (doublet of quartets, $^4J_{HF}$ = 0.5 Hz) assigned to $-CH_2$. The infrared spectrum is as follows: 2940 (w), 1460 (s), 1280 (sh), 1230 (s), 940 (m), 830 (m), 600 (m) cm^{-1}. The mass spectrum contained a molecular ion peak and the appropriate fragmentation pattern.[14]

Reaction of Bis(hexafluoroisopropyl) Sulfite, $((CF_3)_2CHO)_2SO$, with Chlorine Fluoride, ClF. A 75-mL Hoke bomb was charged with 2.5 mmol of $((CF_3)_2CHO)_2SO$ and 10 mmol of ClF and then slowly warmed to -78 °C in a period of 3 h. Warming from -78 °C to room temperature occurred in a period of 12 h. The contents were distilled, and hexafluoroisopropyl fluorosulfate, $(CF_3)_2CHOSO_2F$, was stopped in a trap at -78 °C in about 80% yield. The vapor pressure of this new compound is approximately 60 torr at 25 °C. The ^{19}F NMR spectrum consists of a heptet at ϕ +44.9 ($^4J_{SF-CF_3}$ = 3.7 Hz) and a doublet of doublets at ϕ -72.0 ($^3J_{CF_3-H}$ = 5.5 Hz). The ^1H NMR spectrum shows a heptet at δ 5.2. There was no SF-CH coupling. The infrared spectrum is as follows: 1470 (vs), 1370 (s), 1300 (s), 1250 and 1215 (s, br), 1120 (sh), 1080 (s), 1030 (w), 900 (vs), 880 (s), 840 (vs), 745 (m), 700 (vs), 625 (vs), 600 (s), 545 (s) cm^{-1}. The molecular weight of the compound by *PVT* methods was found to be 254 (calcualted 250). The mass spectrum contained a molecular ion and an appropriate fragmentation pattern.

Reaction of Hexafluoro-2-propanol, $(CF_3)_2CHOH$, with Sulfuryl Chloride Fluoride, SO_2ClF. Hexafluoro-2-propanol (1 mmol) and triethylamine (1 mmol) were condensed into a 50-mL Pyrex reactor equipped with a Teflon stopcock at -196 °C, and the resultant mixture was warmed to room temperature for ~20 min. The mixture was frozen at -196 °C, and the SO_2ClF (1 mmol) was condensed into the reactor. The vessel was then warmed slowly to room temperature and left for ~20 h. The infrared spectrum of the fraction at -78 °C confirmed the formation of $(CF_3)_2CHOSO_2F$ in 50% yield.

Acknowledgment is expressed to the donors of the Petroleum Research Fund, administered by the American Chemical Society, to the National Science Foundation (Grant CHE-8100156), and to the Air Force Office of Scientific Research (Grant 82-0247) for support of this research. Dr. G. D. Knerr obtained the ^{19}F and ^1H NMR and mass spectra.

Registry No. $CF_3CH_2OSO_2F$, 66950-71-8; $EtOSO_2F$, 371-69-7; $(CF_3)_2CHOSO_2F$, 38252-04-9; $(CF_3CH_2O)_2SO$, 53749-89-6; $[(CF_3)_2CHO]_2SO$, 53517-89-8; $(EtO)_2SO$, 623-81-4; ClF, 7790-89-8; XeF_2, 13709-36-9; CF_3CH_2OH, 75-89-8; $(CF_3)_2CHOH$, 920-66-1; SO_2ClF, 13637-84-8.

(14) Sauer, D. T.; Shreeve, J. M. *Inorg. Chem.* **1971**, *10*, 358.
(15) Ahmed, M. G.; Alder, R. W.; James, G. H.; Sinnott, M. L.; Whiting, M. C. *Chem. Commun.* **1968**, 1533.

Contribution from the Departments of Chemistry, University of Florida, Gainesville, Florida 32611, and University of Illinois, Urbana, Illinois 61801

Reinvestigation of the Electronic and Magnetic Properties of Ruthenium Butyrate Chloride

JOSHUA TELSER and RUSSELL S. DRAGO*

Received December 9, 1983

The title compound, hereafter referred to as $Ru_2(but)_4Cl$, was studied by powder magnetic susceptibility measurements over the temperature range 5-300 K, by EPR spectroscopy in various glasses at 4 K, and by far-IR spectroscopy in the solid state at room temperature. The compound has a quartet ground state in agreement with previous reports. A large zero-field splitting (D = 77 cm^{-1}) is found. There is no interdimer magnetic interaction despite the polymeric nature of the solid. EPR spectroscopy gave parameters in agreement with the magnetic data that were independent of the solvent and variation in the axial anion. Unpaired electron spin density was delocalized over both Ru atoms in a series of base adducts. Far-IR spectroscopy showed a band assigned to ν(RuCl) not previously reported. Previous theoretical work is discussed and found to be in agreement with the experimental results.

Introduction

A large number of metal carboxylate dimers are known.[1] One of the most unusual of these is the complex formed with ruthenium, $Ru_2(O_2CR)_4Cl$. In contrast to the metal carboxylate dimers known for Cr, Mo, Re, Tc, Rh, and Cu, this Ru dimer contains an odd number of d electrons. Thus it is formally a $Ru_2^{II,III}$ complex. Structural studies[2] on $Ru_2(but)_4Cl$ (but = butyrate) and other $Ru_2(O_2CR)_4^+$ derivatives[3] indicate that the two Ru atoms are crystallographically equivalent. Furthermore, an earlier report[4] of the magnetic properties and EPR spectra of $Ru_2(but)_4Cl$ gave no support to a localized II,III system. Rather, $Ru_2(but)_4Cl$ was proposed to have a Ru-Ru bond of order 2.5 with three unpaired electrons delocalized over both metal atoms.[2,4] A simplified version of this MO scheme is shown in Figure 1. Scattered-wave Xα calculations have been performed on the $Ru_2(O_2CH)_4^+$ species, and they support this MO scheme.[5] These results have been used with success to explain resonance Raman[6] and single-crystal polarized electronic spectra[7] of $Ru_2(O_2CR)_4^+$ derivatives.

In order to further understanding of this interesting complex, we decided to examine the magnetic properties of $Ru_2(but)_4Cl$ over the temperature interval 5-300 K since the original (powder) measurements were made in the temperature interval 60-300 K.[4] In many cases, magnetic susceptibility measurements are necessary at low temperatures to observe deviation from normal Curie-Weiss behavior. We also decided to repeat the EPR study because, due to a poor signal-to-noise level in the original EPR measurements, a complete spectrum was not obtained and the conclusions are open to question.[4] A complete solution EPR spectrum of the complex and some of its adducts are reported at 4 K. We also obtained far-IR

* To whom correspondence should be addressed at the University of Florida.

(1) Cotton, F. A.; Walton, R. A. "Multiple Bonds Between Metal Atoms"; Wiley-Interscience: New York, 1982, and references therein.
(2) Bennett, M. J.; Caulton, K. G.; Cotton, F. A. *Inorg. Chem.* **1969**, *8*, 1.
(3) Bino, A.; Cotton, F. A.; Felthouse, T. R. *Inorg. Chem.* **1979**, *18*, 2599.
(4) Cotton, F. A.; Pedersen, E. *Inorg. Chem.* **1975**, *14*, 388.
(5) Norman, J. G., Jr.; Renzoni, G. E.; Case, D. A. *J. Am. Chem. Soc.* **1979**, *101*, 5256.
(6) Clark, R. J. H.; Ferris, L. T. H. *Inorg. Chem.* **1981**, *20*, 2759.
(7) Martin, D. S.; Newman, R. A.; Vlasnik, L. M. *Inorg. Chem.* **1980**, *19*, 3404.

0020-1669/84/1323-3114$01.50/0

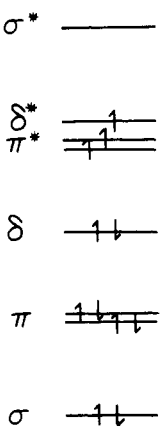

Figure 1. Simplified MO scheme for metal–metal bonding in $Ru_2(O_2CR)_4^+$.

absorption spectra for the complex in the solid state at room temperature.

Experimental Section

Synthesis. $Ru_2(but)_4Cl$ was synthesized from $RuCl_3 \cdot 3H_2O$ (Aldrich) according to the method of Stephenson and Wilkinson.[8] The complex was recrystallized twice from butyric acid. Anal. Calcd for $Ru_2C_{16}H_{28}O_8Cl$: C, 32.79; H, 4.82; Cl, 6.05. Found: C, 32.65; H, 4.80; Cl, 5.98.

Magnetic Susceptibilities. Magnetic susceptibility measurements were performed on an SHE Corp. (San Diego, CA) VTS-50 SQUID magnetometer (Department of Physics, University of Illinois). Ten measurements were recorded at each temperature at a field of 10.0 kG with the mean and standard deviation directly calculated. Hg[Co(NCS)$_4$] was used to check the instrument, and the susceptibility value obtained agreed with the literature value.

EPR Spectra. EPR spectra were recorded on a Bruker ER-200D X-band instrument equipped with an Oxford liquid-helium cryostat (Department of Physics, University of Illinois). The magnetic field was previously calibrated and the microwave frequency measured by a Systron Donner Model 6245A instrument. Samples were $\sim 1 \times 10^{-2}$ M in sealed, degassed quartz tubes.

Computer Simulations. Computer simulations were performed on a VAX 11/780 computer. For the magnetic susceptibility data the master program DSUSFIT was used.[9] The program uses the nonlinear least-squares fitting program DSTEPIT.[10] For the EPR simulations the program QPOW was used.[11] In the simulations done here, the frame of reference was chosen so that the **g** tensor is diagonal (with $g_x = g_y = g_\perp$) and the **A** tensor was held in the same orientation as the **g** tensor. The nuclear **g** tensor was approximated as an isotropic $g_N = \mu_N/I$.

Far-Infrared Spectra. Far-IR spectra were obtained on a Digilab Fourier transform IR spectrometer. $Ru_2(but)_4Cl$ was prepared as a CsI pellet (1% w/w).

Data and Theory. The magnetic susceptibility of a powder sample of $Ru_2(but)_4Cl$ was determined over the temperature range 5–300 K. Most data points were taken at low temperatures since the magnetic susceptibility of $Ru_2(but)_4Cl$ had not been previously reported below 60 K. Initially, the data were least-squares fitted to a Curie–Weiss law behavior curve, $1/\chi = a_0 + a_1 T$. The points ≥ 35 K fitted well to this equation (correlation 0.999 98) to give values that agree closely with those reported[4] (see Table I). Our value for χ_M^{300} (6.852×10^{-3}) is much closer to the solution value obtained from both the Gouy and Evans methods (6.91×10^{-3}) than is the previously reported powder value (6.74×10^{-3}).[4] This agreement of the solution and solid-state values is supported by the computer simulations that show insignificant interdimer interactions (vide infra). Thus, at temperatures ≥ 35 K, $Ru_2(but)_4Cl$ exhibits normal paramagnetic behavior with a positive Weiss constant. A diamagnetic correction of -278×10^{-6} cgsu was used,[4] and it is simply the value obtained from Pascal's constants including the underlying diamagnetism of Ru(II) and Ru(III).[12] The data below 35 K did not fit the Curie–Weiss law as well since high-temperature approximations are no longer valid. In order to correctly explain these data, a full exponential treatment was needed. Several models are reasonable since in $Ru_2(but)_4Cl$ there may be both intramolecular and intermolecular effects. The latter is due to the polymeric nature of the solid-state structure of $Ru_2(but)_4Cl$ wherein $Ru_2(but)_4^+$ units are bridged by chlorides to form an infinite linear chain.[2] Thus intermolecular antiferromagnetic exchange between Ru dimers is possible. Furthermore, as with all $S > {}^1/_2$ states, zero-field splitting within the Ru dimer ($S = {}^3/_2$) is possible and this is an "intramolecular antiferromagnetic" effect. These data were fitted to five models in an attempt to separate these effects and understand the magnetic behavior of $Ru_2(but)_4Cl$.

Table I. High-Temperature Powder Magnetic Susceptibility Data on $Ru_2(but)_4Cl$

	a_0	a_1	C	θ	g	$10^3 \chi_M^{300}$, cgsu
ref 4 (60–300 K)	6.6	0.472	2.12	14	2.13	6.74 ± 0.03 6.91 ± 0.05 (in solns)
this work (35–300 K)	6.984	0.4632	2.16	15.1	2.15	6.852 ± 0.003

The first used was the full spin Hamiltonian for an O_h $S = {}^3/_2$ system:

$$\mathcal{H} = \beta(g_x H_x S_x + g_y H_y S_y + g_z H_z S_z) + D[S_z^2 - {}^1/_3 S(S+1)] + E(S_x^2 - S_y^2)$$

D and E are scalar crystal field splitting parameters. With only axial distortion, $E = 0$ and $g_x = g_y = g_\perp$. The matrix elements for this Hamiltonian are given in Table V. The second model used was the exponential form for the zero-field susceptibility of an O_h $S = {}^3/_2$ complex with axial zero-field splitting. The equations are taken from O'Connor:[13]

$$\chi_\parallel = \frac{N g_\parallel^2 \beta^2}{kT} \frac{1 + 9\exp(-2D/kT)}{4(1 + \exp(-2D/kT))}$$

$$\chi_\perp = \frac{N g_\perp^2 \beta^2}{kT} \frac{4 + (3kT/D)(1 - \exp(-2D/kT))}{4(1 + 2\exp(-2D/kT))}$$

An orientation average, $\chi_{av} = (\chi_\parallel + 2\chi_\perp)/3$, was used. The third model used was the Ising model, which considers a one-dimensional infinite chain of antiferromagnetically coupled spins. The full exponential form for the zero-field susceptibility for $S = {}^3/_2$ has been worked out by Suzuki, Tsujiyama, and Katsura.[14] The equation is quite lengthy and will not be reproduced here. It makes no provision for effects other than an antiferromagnetic interaction along the linear chain. Once again, on the basis of the crystal structure of $Ru_2(but)_4Cl$ this model is not unreasonable since there is an infinite approximately linear chain of chloride-bridged $Ru_2(but)_4^+$ units.

The fourth and fifth models used were attempts to include both intramolecular zero-field splitting and intermolecular antiferromagnetic exchange. One method was to include intermolecular effects with use of the molecular field approximation.[13] The parameter zJ was included to account for weak magnetic interactions between $S = {}^3/_2$ units. The equation is

$$\chi_i' = \frac{\chi_i}{1 - (2zJ/Ng_i^2\beta^2)\chi_i}$$

(8) Stephenson, T. A.; Wilkinson, G. *J. Inorg. Nucl. Chem.* **1966**, *28*, 2285.
(9) (a) Lambert, S. L.; Spiro, C. L.; Gagnē, R. R.; Hendrickson, D. N. *Inorg. Chem.* **1982**, *21*, 68. (b) Laskowski, E. J.; Hendrickson, D. N. *Inorg. Chem.* **1978**, *17*, 457. (c) Lambert, S. L. Ph.D. Thesis, University of Illinois, 1981. (d) Laskowski, E. J. Ph.D. Thesis, University of Illinois, 1976.
(10) Chandler, J. P. Quantum Chemistry Program Exchange, Indiana University, Bloomington, IN, 1965; Program 66.
(11) Liczwek, D. L.; Belford, R. L.; Pilbrow, J. R.; Hyde, J. S. *J. Phys. Chem.* **1983**, *87*, 2509. Nilges, M. J. Ph.D. Thesis, University of Illinois, 1979. Altman, T. E. Ph.D. Thesis, University of Illinois, 1981. Maurice, A. M. Ph.D. Thesis, University of Illinois, 1982.
(12) Mulay, L. N. "Magnetic Susceptibility"; Wiley-Interscience: New York, 1963.
(13) O'Connor, C. J. *Prog. Inorg. Chem.* **1982**, *29*, 203 and references therein.
(14) Suzuki, M.; Tsujiyama, B.; Katsura, S. *J. Math. Phys. (N.Y.)* **1967**, *8*, 124.

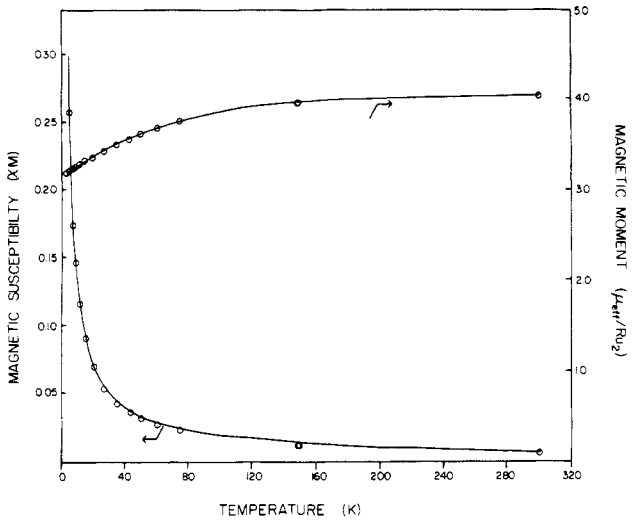

Figure 2. Molar paramagnetic susceptibility and effective magnetic moment per $Ru_2(but)_4Cl$ molecule vs. temperature. The solid lines result from a least-squares fit to the theoretical equation for a $S = {}^3/_2$ complex with axial zero-field splitting.

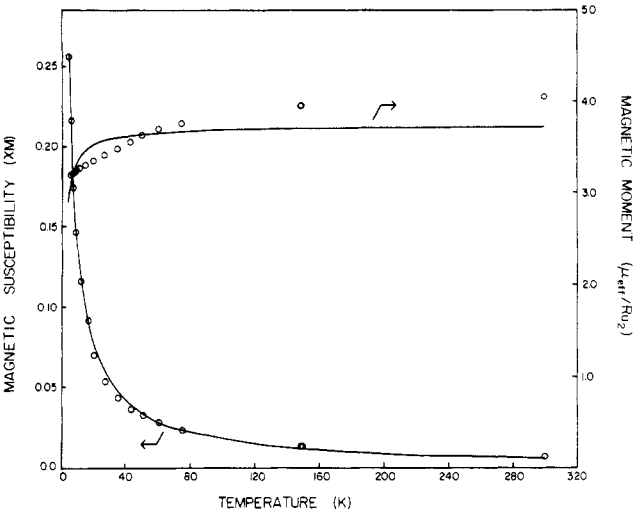

Figure 3. Molar paramagnetic susceptibility and effective magnetic moment per $Ru_2(but)_4Cl$ molecule vs. temperature. The solid lines result from a least-squares fit to the theoretical equation for an infinite chain of antiferromagnetic exchange coupled $S = {}^3/_2$ units (Ising model).

where $\chi_i = \chi_\parallel$ or $\chi_\perp$, $g_i = g_\parallel$ or $g_\perp$, and the equations for χ_i are those given in method 2.

The final approach was to use as a model a dimer of $S_1 = S_2 = {}^3/_2$ units that are antiferromagnetically coupled, with both S_1 and S_2 undergoing the same axial zero-field splitting. This model only treats interactions between a pair of $Ru_2(but)_4^+$ units and ignores any longer range interactions. To develop a model including longer range interactions by using a trimer (either linear or joined) or higher polymers and including zero-field splitting on all the units would be very complex. Hendrickson and Laskowski[9b,d] have studied an $S_1 = S_2 = {}^5/_2$ dimer with axial zero-field splitting on both S_1 and S_2 using the spin Hamiltonian

$$\mathcal{H} = g_\parallel\beta\mathbf{H}_z\cdot\mathbf{S}_z + g_\perp\beta(\mathbf{H}_x\cdot\mathbf{S}_x + \mathbf{H}_y\cdot\mathbf{S}_y) + D[\mathbf{S}_z^2 - {}^1/_3S(S+1)] - 2J\mathbf{S}_1\cdot\mathbf{S}_2$$

In this equation a coupled basis set, $S = S_1 + S_2$, is used[15] (see Table VI). D is the axial zero-field splitting parameter. J is an isotropic exchange parameter (Heisenberg–Dirac–Van Vleck form). Only an isotropic J is needed since S_1 and S_2 are symmetry related. The matrix elements for this spin Hamiltonian are given in Table VII.

Results

Magnetic Susceptibility. The first two zero-field splitting models described in the Experimental Section fit the data reasonably well. The parameters obtained by computer simulations of the magnetic data (method 1) gave the best fit and g values that compare most closely to those obtained from the EPR spectra of $Ru_2(but)_4Cl$ in various solvents (vide infra). The experimental and theoretical curves for χ_M and μ_{eff} are shown in Figure 2. The value obtained for D, 77 cm^{-1}, is fairly large. In transition-metal complexes D is dominated by spin–orbit coupling effects.[13] These effects depend on the atomic number of the paramagnetic center and on the interaction of ground and excited electronic states. Both of these effects would be large for $Ru_2(but)_4Cl$, which has two second-row transition metals and a large number of closely spaced electronic states. Few calculations have been performed to theoretically determined D values;[16] $Ru_2(but)_4Cl$ is no doubt far too complex, and there are no analogous compounds with which to compare this value. Conventional EPR spectroscopy has been used to measure D for a number of high-spin molecules;[16,17] however, commonly used microwave frequencies do not exceed ~3 cm^{-1}, far too small to determine D in this complex. Use of far-infrared magnetic resonances, which can go up to several hundred reciprocal centimeters, would allow an independent determination of D to compare with the above values. This method has been used successfully to study metalloporphyrins with large zero-field splitting.[18] The exponential form for the zero-field susceptibility (method 2) fits the experimental data well but gave $g_\parallel$ in poor agreement with the EPR data. One would expect use of the full spin Hamiltonian with the experimental magnetic field to determine the energy levels more accurately than the zero-field exponential model. Thus method 2 is qualitatively correct, but method 1 is quantitatively better. By contrast, using the other extreme, the Ising model (method 3), which only considers antiferromagnetic exchange between $S = {}^3/_2$ units, one obtains a very poor fit to the data (see Figure 3). A g_{av} value of 1.93 is obtained with $J = -0.32$ cm^{-1}. Since the fit is so poor, these values have little meaning.

Table II. Parameters Obtained from Computer Simulation of the Powder Magnetic Susceptibility Data (Full Temperature Range) Using the Models Described in the Text

method	D^a	J^a	$g_\parallel$	$g_\perp$	g_{av}	$zJ_\parallel{}^a$	$zJ_\perp{}^a$	SE[b]
1[c]	76.8		2.02	2.14	2.10			0.0038
2	57.7		3.03	1.96	2.32			0.13
3		−0.0316			1.93			0.16
4	65.6		2.94	2.01	2.32	1.98	−0.250	0.11
5	0.212	−1.15	2.06	3.19	2.81			0.097

[a] Values in cm^{-1}. [b] SE, the standard error of estimate, is a measure of the goodness of fit of the model to the data.[25] SE = $[\Sigma_{i=1}^{n}((\mu_{eff})_i^{obsd} - (\mu_{eff})_i^{calcd})^2/(n-k)]^{1/2}$, where n is the number of data points and k is the number of varying parameters. [c] The method of choice (see text). Values are accurate to ±5%.

Use of method 4, which contained zJ parameters to include both zero-field splitting and exchange effects, was also unsuccessful. These parameters did not improve the fit and gave unreasonable values. A more exact treatment in which the full spin Hamiltonian for a dimer of $S = {}^3/_2$ units experiencing zero-field splitting was used (method 5). Once again, the fit was very poor and the values obtained were of little meaning (see Table II). This is not surprising since the model assumes

(15) Condon, E. V.; Shortley, G. H. "The Theory of Atomic Spectra"; Cambridge University Press: New York, 1963.
(16) Weltner, W., Jr. "Magnetic Atoms and Molecules"; Van Nostrand-Reinhold: New York, 1983, and references therein.
(17) Van Zee, R. J.; Brown, C. M.; Zeringue, K. J.; Weltner, W., Jr. *Acc. Chem. Res.* **1980**, *13*, 237 and references therein.
(18) Brackett, G. C.; Richards, P. L.; Caughey, W. S. *J. Chem. Phys.* **1971**, *54*, 4383.

Table III. Parameters Obtained from Computer Simulation of Frozen-Solution EPR Spectra of $Ru_2(but)_4Cl$

	$g_\parallel$	$g_\perp$	g_{av}	$10^4A_\parallel$[a]	$10^4A_\perp$[a]
ref 4 (methanol, 4.2 K, 9.186 GHz)	2.03	2.18	2.13	9 ± 3	31
this work (1:1 toluene/CH_2Cl_2, 3.4 K, 9.4450 GHz)	1.9465 ± 0.0005	2.200 ± 0.001	2.12	21.7 ± 0.5	26.7 ± 0.5

[a] Values in cm^{-1}.

Table IV. Experimental and Calculated Magnetic Susceptibility Data

temp, K	$10^3\chi_M$ (exptl), cgsu	$10^6\sigma$, cgsu	$10^3\chi_M$(calcd), cgsu, methods 1	2	3	4	5	μ_{eff} (exptl), μ_B	μ_{eff}(calcd), μ_B, methods 1	2	3	4	5
299.30	6.855	3.4	6.838	6.948	5.790	6.916	7.627	4.0535	4.0483	4.0809	3.7254	4.0716	4.2757
148.60	13.243	12.3	13.278	13.152	11.589	13.168	12.823	3.9672	3.9725	3.9535	3.7111	3.9560	3.9038
147.90	13.272	12.1	13.335	13.207	11.643	13.224	12.872	3.9622	3.9616	3.9524	3.7110	3.9549	3.9020
74.40	23.942	14.2	23.957	23.813	22.799	23.875	23.006	3.7744	3.7756	3.7642	3.6832	3.7691	3.6999
74.20	24.050	23.4	24.009	23.867	22.858	23.928	23.060	3.7778	3.7746	3.7634	3.6830	3.7682	3.6993
60.08	28.606	25.5	28.422	28.412	28.030	28.447	27.821	3.7074	3.6955	3.6949	3.6699	3.6971	3.6562
59.98	28.645	12.5	28.459	28.451	28.975	28.485	27.833	3.7069	3.6948	3.6943	3.6898	3.6965	3.6559
50.00	33.084	11.9	32.893	33.002	33.429	32.998	32.833	3.6373	3.6267	3.6328	3.6561	3.6325	3.6234
42.90	37.072	3.6	37.195	37.371	38.674	37.337	37.744	3.5664	3.5723	3.5808	3.6426	3.5791	3.5986
35.01	43.724	15.3	43.920	44.114	46.837	44.059	45.472	3.4989	3.5069	3.5144	3.6214	3.5123	3.5682
34.99	43.754	15.3	43.941	44.132	46.862	44.078	45.496	3.4991	3.5066	3.5142	3.6213	3.5121	3.5681
27.00	54.443	31.4	54.675	54.766	59.600	54.726	57.763	3.4287	3.4360	3.4389	3.5875	3.4376	3.5317
20.00	70.698	45.9	71.064	70.934	78.194	70.925	76.140	3.3628	3.3715	3.3684	3.5366	3.3682	3.4898
15.00	91.801	44.1	92.069	91.692	100.53	91.666	98.989	3.3168	3.3234	3.3166	3.4728	3.3161	3.4460
11.50	117.19	27.5	117.59	116.96	125.50	116.84	125.59	3.2830	3.2876	3.2798	3.3975	3.2781	3.3986
9.00	147.27	92.4	147.59	147.04	152.31	146.79	155.47	3.2558	3.2594	3.2533	3.3111	3.2505	3.3452
7.50	175.19	63.0	175.00	174.72	174.41	174.41	181.20	3.2416	3.2398	3.2373	3.2344	3.2344	3.2967
6.00	216.74	78.7	215.52	216.23	203.38	216.21	216.59	3.2250	3.2159	3.2212	3.1240	3.2210	3.2239
5.00	257.40	156.7	255.22	257.74	227.88	258.80	248.15	3.2083	3.1946	3.2104	3.0187	3.2170	3.1501

that antiferromagnetic exchange is the dominant term in the spin Hamiltonian whereas with $Ru_2(but)_4Cl$ it is zero-field splitting that is dominant, if not the sole field-independent term in the Hamiltonian. There are of course problems inherent to applying this dimer model to the polymeric $Ru_2(but)_4Cl$. Also, the validity of the use of the Heisenberg Hamiltonian in dimers in which both units are paramagnetic has been recently questioned.[19] However, it was found that for such systems in which the valences are localized the Heisenberg Hamiltonian is still valid. This is most likely the case for $Ru_2(but)_4Cl$ since the Ru_2 units are quite widely separated and the interaction is small if it exists at all. The conclusion that can be drawn from the magnetic susceptibility data is that $Ru_2(but)_4Cl$, in spite of its polymeric structure, is a complex in which the $Ru_2(but)_4^+$ units can be treated as isolated $S = {}^3/_2$ systems. This is in agreement with the EPR data (vide infra) and with the crystallographic data since the Ru–Cl bond is extremely long[2] (2.587 vs. 2.35 Å in Ru(III) chloride complexes[20]), indicating a weak interaction. The experimental and calculated values for χ_M and μ_{eff} are given in Table IV.

EPR Spectra. The EPR Spectrum of $Ru_2(but)_4Cl$ in various solvent systems was obtained at liquid-helium temperatures. No spectrum could be observed at 77 K, although Cotton and Pedersen[4] report a broad signal at this temperature. We also could not observe an EPR spectrum for pure powder $Ru_2(but)_4Cl$ at 4 K, presumably because of magnetic exchange interactions leading to fast electron spin relaxation. The following spin Hamiltonian is used to interpret the EPR spectrum:

$$\mathcal{H} = \beta\mathbf{H}\cdot\mathbf{g}\cdot\mathbf{S} + \mathbf{I}\cdot\mathbf{A}\cdot\mathbf{S} - \beta_N\mathbf{H}\cdot\mathbf{g}_N\cdot\mathbf{I} + \mathbf{S}\cdot\mathbf{D}\cdot\mathbf{S}$$

Since the value for D is large ($\sim$77 cm^{-1}) only the $M_S = \pm{}^1/_2$ state is populated at 4 K and the microwave frequency is too small ($\sim$0.3 cm^{-1}) to effect any transitions to the $M_S = \pm{}^3/_2$ states. Thus a computer simulation of the frozen-solution spectra could be performed by using a program for powder pattern spectra of $S = {}^1/_2$ systems. Ruthenium has five zero-spin nuclei (^{96}Ru, ^{98}Ru, ^{100}Ru, ^{102}Ru, and ^{104}Ru) and two nuclei with $I = {}^5/_2$: ^{99}Ru, $\mu = -0.63$, 12.72% natural abundance; ^{101}Ru, $\mu = -0.69$, 17.07% natural abundance. The simulations treat the $I = {}^5/_2$ nuclei individually using their own g_N values (the same g and A values), and the two are added in the correct isotopic ratio. The spectrum for the zero-spin nuclei (only electronic Zeeman terms) is determined independently and can then be added to the $I = {}^5/_2$ spectrum in the desired ratio. The EPR spectrum of $Ru_2(but)_4Cl$ in 1:1 toluene/CH_2Cl_2 with 1% v/v acetone showing both the parallel and perpendicular regions is shown in Figure 4. The perpendicular and parallel regions (the latter in 9:1 methanol/ethanol) are shown independently on an expanded scale in Figures 5 and 6, respectively. The values obtained by computer simulation of the spectra are given in Table III. The simulations gave $g_\perp = 4.40$ for an $S = {}^1/_2$ system. For an $S = {}^3/_2$ system with $D >> g\beta H$ one can refer to effective g values, $g^e = h\nu/\beta H$, such that, for the $M_S = \pm{}^1/_2$ Kramers doublet, $g_\parallel{}^e \simeq g_\parallel$ and $g_\perp{}^e \simeq 2g_\perp[1 - (3/16)(g_\perp\beta H/D)^2]$.[16] For D as large as it is in this complex, $g_\perp{}^e \simeq 2g_\perp$. Thus $g_\perp = 2.200$, close to the value obtained by Cotton and Pedersen.[4] The value for $g_\parallel$ (1.9465) also differs slightly from theirs (2.03), but they did not actually observe the parallel signals at 4 K. Our value obtained for $A_\perp$ was 26.7×10^{-4} cm^{-1} and for $A_\parallel$ was 21.7

Table V. Upper-Right-Hand Non-Zero Matrix Elements for Spin Hamiltonian Used in Method 1[a]

$$\langle S, m_S|\mathcal{H}|S_1M_S\rangle = \langle 3/2, +3/2|\mathcal{H}|3/2, +3/2\rangle = (3/2)g_\parallel\beta H_\parallel + 9D/4 \text{ (or } +D)$$
$$= \langle 3/2, +3/2|\mathcal{H}|3/2, +1/2\rangle = (3/2)^{1/2}g_\perp\beta H_\perp$$
$$= \langle 3/2, +1/2|\mathcal{H}|3/2, +1/2\rangle = (1/2)g_\parallel\beta H_\parallel + D/4 \text{ (or } -D)$$
$$= \langle 3/2, +1/2|\mathcal{H}|3/2, -1/2\rangle = g_\perp\beta H_\perp$$
$$= \langle 3/2, -1/2|\mathcal{H}|3/2, -1/2\rangle = -(1/2)g_\parallel\beta H_\parallel + D/4 \text{ (or } -D)$$
$$= \langle 3/2, -1/2|\mathcal{H}|3/2, -3/2\rangle = (3/2)^{1/2}g_\perp\beta H_\perp$$
$$= \langle 3/2, -3/2|\mathcal{H}|3/2, -3/2\rangle = -(3/2)g_\parallel\beta H_\parallel + 9D/4 \text{ (or } +D)$$

[a] The constant term $-{}^1/_3S(S+1)$ was not included; inclusion leads to $\pm D$ rather than $9D/4$ or $D/4$.

(19) Girerd, J.-J. *J. Chem. Phys.* **1983**, *79*, 1766.
(20) Hopkins, T. E.; Zalkin, A.; Templeton, D. H.; Adamson, M. G. *Inorg. Chem.* **1966**, *5*, 1427, 1431.

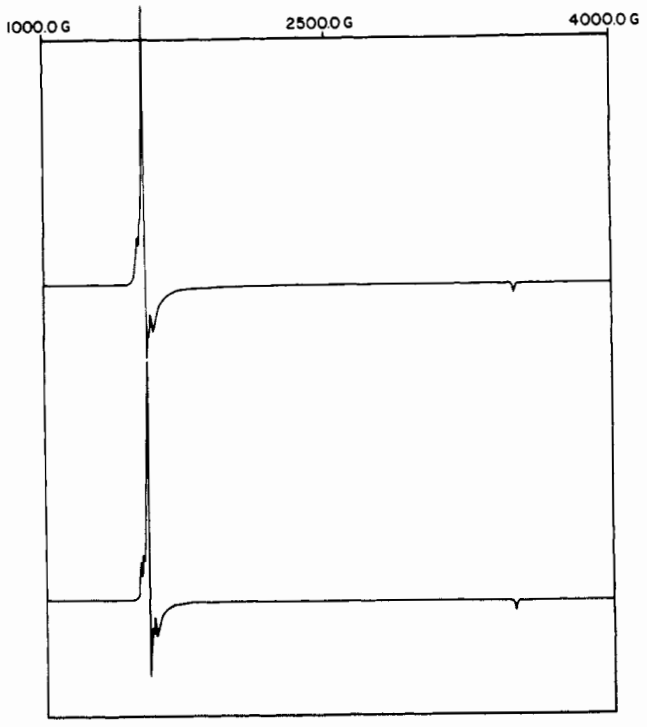

Figure 4. Top: Computer EPR spectrum of $Ru_2(but)_4Cl$ ($\sim 1 \times 10^{-2}$ M) in 1:1 toluene/CH_2Cl_2 with 1% v/v acetone at 3.4 K and 9.4450 GHz. Bottom: Computer simulation of the above using 54.09% $S = {}^1/_2$, $I = 0$, $g_\parallel = 1.9465$, $g_\perp = 4.400$ and 45.91% $S = {}^1/_2$, $I = {}^5/_2$, unchanged g values, $A_\parallel = 21.7 \times 10^{-4}$ cm^{-1}, $A_\perp = 26.7 \times 10^{-4}$ cm^{-1} (43% $\mu = -0.63$, 57% $m = -0.69$, A values calcualted for the former). Single-molecule spectra with Lorentzian line widths (half-width at half-height) of 40 MHz in the perpendicular region and 10 MHz in the parallel region were added for every step of 1.0° in the polar angle θ.

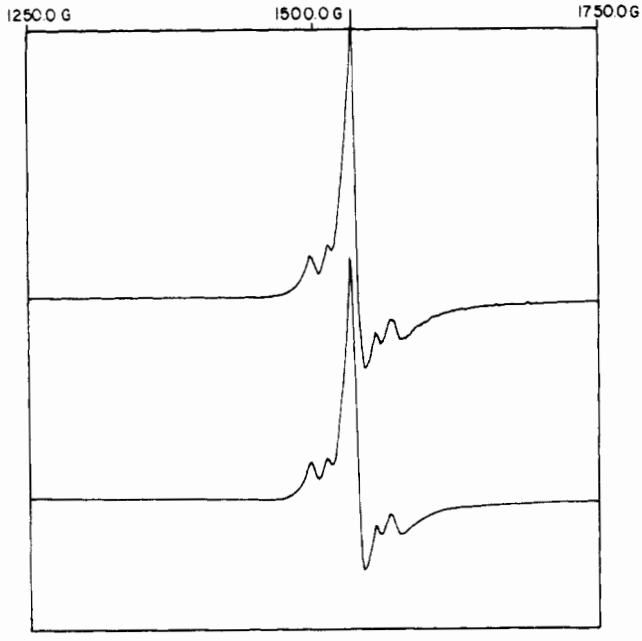

Figure 5. Top: EPR spectrum of $Ru_2(but)_4Cl$ showing the perpendicular region only. Bottom: Computer simulation of the above using the parameters given in Figure 4.

$\times 10^{-4}$ cm^{-1} (A values for $\mu = -0.63$). This differs considerably from the previously reported value ($9 (\pm 3) \times 10^{-4}$ cm^{-1}); our value, however, is based on an observed spectrum. The EPR parameters and relative intensities of the zero-spin to $I = {}^5/_2$ signals were solvent independent. The line widths did vary somewhat with solvent. The narrower line widths in 1:1 toluene/CH_2Cl_2 allowed better resolution of the perpendicular region but led to extensive noise in the parallel region. The

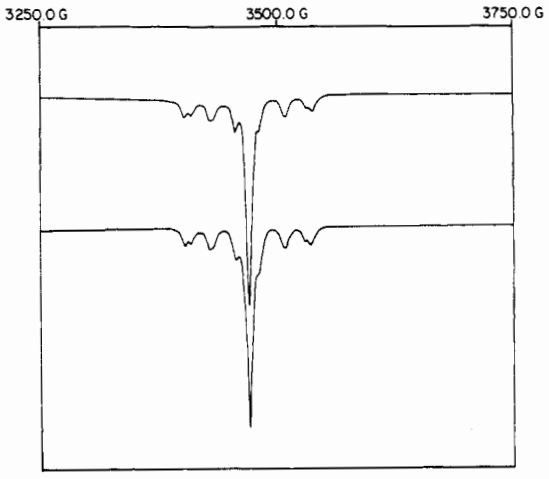

Figure 6. Top: EPR spectrum of $Ru_2(but)_4Cl$ showing the parallel region only in 9:1 methanol/ethanol at 9.4478 GHz. Bottom: Computer simulation of the above using the parameters given in Figure 4 except with line widths of 90 MHz in the perpendicular region.

Table VI. Coupled Basis Set for $S = S_1 + S_2$ Where $S_1 = S_2 = {}^3/_2$, Used in Method 5[a]

$|S, M_S\rangle = |M_{S_1}, M_{S_2}\rangle$

$|3, \pm 3\rangle = |\pm 3/2, \pm 3/2\rangle$

$|3, \pm 2\rangle = (1/2^{1/2})|\pm 3/2, \pm 1/2\rangle + (1/2^{1/2})|\pm 1/2, \pm 3/2\rangle$

$|3, \pm 1\rangle = (1/5^{1/2})|\pm 3/2, \mp 1/2\rangle + (1/5^{1/2})|\pm 1/2, \pm 3/2\rangle + (3/5)^{1/2}|\pm 1/2, \pm 1/2\rangle$

$|3, 0\rangle = (1/20^{1/2})|+3/2, -3/2\rangle + (1/20^{1/2})|-3/2, +3/2\rangle + (9/20)^{1/2}|+1/2, -1/2\rangle + (9/20)^{1/2}|-1/2, +1/2\rangle$

$|2, \pm 2\rangle = \pm(1/2^{1/2})|\pm 3/2, \pm 1/2\rangle \mp (1/2^{1/2})|\pm 1/2, \pm 3/2\rangle$

$|2, \pm 1\rangle = \pm(1/2^{1/2})|\pm 3/2, \mp 1/2\rangle \mp (1/2^{1/2})|\mp 1/2, \pm 3/2\rangle$

$|2, 0\rangle = (1/2)|+3/2, -3/2\rangle - (1/2)|-3/2, +3/2\rangle + (1/2)|+1/2, -1/2\rangle - (1/2)|-1/2, +1/2\rangle$

$|1, \pm 1\rangle = (3/10)^{1/2}|\pm 3/2, \mp 1/2\rangle + (3/10)^{1/2}|\mp 1/2, \pm 3/2\rangle - (4/10)^{1/2}|\pm 1/2, \pm 1/2\rangle$

$|1, 0\rangle = (9/20)^{1/2}|+3/2, -3/2\rangle + (9/20)^{1/2}|-3/2, +3/2\rangle - (1/20^{1/2})|+1/2, -1/2\rangle - (1/20^{1/2})|-1/2, +1/2\rangle$

$|0, 0\rangle = (1/2)|+3/2, -3/2\rangle - (1/2)|-3/2, +3/2\rangle - (1/2)|+1/2, -1/2\rangle + (1/2)|-1/2, +1/2\rangle$

[a] Derived with use of ref 15.

Table VII. Upper-Right-Hand Non-Zero Matrix Elements for Spin Hamiltonian Used in Method 5

$\langle S, M_S|\mathcal{H}|S, M_S\rangle = \langle 3, \pm 3|\mathcal{H}|3, \pm 3\rangle = -12J + 9D/2 \pm 3g_\parallel\beta H_\parallel$
$= \langle 3, \pm 2|\mathcal{H}|3, \pm 2\rangle = -12J + 5D/2 \pm 2g_\parallel\beta H_\parallel$
$= \langle 3, \pm 1|\mathcal{H}|3, \pm 1\rangle = -12J + 13D/10 \pm g_\parallel\beta H_\parallel$
$= \langle 3, 0|\mathcal{H}|3, 0\rangle = -12J + 9D/10$
$= \langle 2, \pm 2|\mathcal{H}|2, \pm 2\rangle = -6J + 5D/2 \pm 2g_\parallel\beta H_\parallel$
$= \langle 2, \pm 1|\mathcal{H}|2, \pm 1\rangle = -6J + 5D/2 \pm g_\parallel\beta H_\parallel$
$= \langle 2, 0|\mathcal{H}|2, 0\rangle = -6J + 5D/2$
$= \langle 1, \pm 1|\mathcal{H}|1, \pm 1\rangle = -2J + 17D/10 \pm g_\parallel\beta H_\parallel$
$= \langle 1, 0|\mathcal{H}|1, 0\rangle = -2J + 41D/10$
$= \langle 0, 0|\mathcal{H}|0, 0\rangle = 5D/2$
$= \langle 3, \pm 1|\mathcal{H}|1, \pm 1\rangle = 24^{1/2}D/5$
$= \langle 3, 0|\mathcal{H}|1, 0\rangle = 6D/5$
$= \langle 2, 0|\mathcal{H}|0, 0\rangle = 2D$
$= \langle 3, 3|\mathcal{H}|3, 2\rangle = (3/2)^{1/2}g_\perp\beta H_\perp$
$= \langle 3, 2|\mathcal{H}|3, 1\rangle = (5/2)^{1/2}g_\perp\beta H_\perp$
$= \langle 3, 1|\mathcal{H}|3, 0\rangle = 3^{1/2}g_\perp\beta H_\perp$
$= \langle 3, -1|\mathcal{H}|3, -2\rangle = (5/2)^{1/2}g_\perp\beta H_\perp$
$= \langle 3, -2|\mathcal{H}|3, -3\rangle = (3/2)^{1/2}g_\perp\beta H_\perp$
$= \langle 2, 2|\mathcal{H}|2, 1\rangle = g_\perp\beta H_\perp$
$= \langle 2, 1|\mathcal{H}|2, 0\rangle = (3/2)^{1/2}g_\perp\beta H_\perp$
$= \langle 2, 0|\mathcal{H}|2, -1\rangle = (3/2)^{1/2}g_\perp\beta H_\perp$
$= \langle 2, -1|\mathcal{H}|2, -2\rangle = g_\perp\beta H_\perp$
$= \langle 1, 1|\mathcal{H}|1, 0\rangle = 1/2^{1/2}g_\perp\beta H_\perp$
$= \langle 1, 0|\mathcal{H}|1, -1\rangle = 1/2^{1/2}g_\perp\beta H_\perp$

broader line widths in 9:1 methanol/ethanol gave less noise in the parallel region. The relative intensities of the zero-spin to $I = {}^5/_2$ signals in all solvent systems corresponded to 45.91% with $I = {}^5/_2$ and 54.09% with $I = 0$. This is the ratio that would be expected for delocalization over both Ru atoms. For a Ru dimer, 49.29% of the dimers will have two zero-spin Ru nuclei, 41.83% will have one $I = {}^5/_2$ Ru nucleus, and 8.87% will have two $I = {}^5/_2$ nuclei. The last type will give a signal of very low intensity since not only will there be few such dimers but the transitions will also be spread out over 11 lines. Delocalization was proposed[4] earlier for $Ru_2(but)_4Cl$, but since only a rather broad signal in the perpendicular region and none in the parallel region was observed, there is some question concerning the validity of their conclusions. Our observation of the parallel signal, which has much narrower line widths and larger hyperfine splitting (in G) than the perpendicular signal, allows this delocalization to be unequivocally determined. Furthermore, in the toluene/CH_2Cl_2 glass the perpendicular line widths are much narrower than in the previous work. This allows the relative intensities in that area of the spectrum to be more clearly determined. To investigate this delocalization as a function of solvent, anion, and added bases, other spectra were obtained. A totally symmetric species, for example $[Ru_2(but)_4(MeOH)_2](CF_3SO_3)$, would be expected to contain equivalent ruthenium atoms but an asymmetric complex such as $[Ru_2(but)_4(donor)Cl]$ might not. The effect of chloride coordination was investigated by generating $[Ru_2(but)_4(MeOH)_2](CF_3SO_3)$ in solution by addition of 1 equiv of $Ag(CF_3SO_3)$ to a solution of $Ru_2(but)_4Cl$ in 9:1 methanol/ethanol, leading to precipitation of AgCl. The species in solution is presumably $[Ru_2(but)_4(MeOH)_2](CF_3SO_3)$ since $CF_3SO_3^-$ is such a poorly coordinating anion. The EPR spectrum of this species is identical with that obtained for $Ru_2(but)_4Cl$ in methanol/ethanol, indicating extensive chloride ion dissociation in agreement with conductivity results.[8] The parameters and relative intensities were the same for the triflate as for $Ru_2(but)_4Cl$ in 1:1 toluene/CH_2Cl_2 with 1% acetone, in which the complex exists most likely as $(CH_3)_2CO{\cdot}Ru_2(but)_4Cl$. Acetone (even in excess) is not expected to displace chloride in such a low-dielectric-constant medium.[21] Furthermore, a solution of $Ru_2(but)_4Cl$ in 1:1 toluene/CH_2Cl_2 with only 1 equiv of pyridine added gave an EPR spectrum similar to that for acetone. In this low-dielectric-constant solvent the predominant species is most likely $[Ru_2(but)_4(py)Cl]$. The main difference in the EPR spectra occurs when the solvent is changed from 1:1 toluene/CH_2Cl_2 to 9:1 methanol/ethanol. The line width in the perpendicular region is sharper in the former solvent because it forms a better glass and has a lower dielectric constant.

The EPR spectra can provide information regarding equivalence of the ruthenium atoms. If complete localization of unpaired electron spin density occurred, one would observe an intensity ratio of 70.21% for the signal arising from spin on an $I = 0$ nucleus to 29.79% for that on a $I = {}^5/_2$ nucleus. As expected, this result was never observed for it is unreasonable to expect localization to this extent in a strongly metal–metal-bonded complex. Delocalization of unpaired electron spin density over both metal atoms has been found unequivocally in analogous paramagnetic metal carboxylate dimers of Mo,[22] Re,[23] and Rh.[24] When complete electron delocalization exists, the relative intensities of zero-spin to $I = {}^5/_2$ signals will be 54.09% to 45.91%. This was the observed result. However, this result does not prove that the two ruthenium atoms are chemically equivalent. For nonequivalent nuclei, the hyperfine pattern would show different A values for the chloride-bound Ru vs. the pyridine-bound Ru in $[Ru_2(but)_4(py)Cl]$. Given the experimental line widths in the parallel region of 3.34×10^{-4} cm^{-1}, the difference in A values must be considerably less than this since only one A value could be resolved. Thus the question of the equivalence of electron delocalization over the Ru atoms cannot be completely answered without the use of isotopically pure ruthenium. Natural-abundance Ru is dominated by the many zero-spin isotopes, which give no information on chemical equivalence, and the low abundance of the two $I = {}^5/_2$ nuclei makes resolution of slight changes in A values impossible. In contrast, isotopically pure complexes would show either an 11-line spectrum in a 1:2:3:4:5:6:5:4:3:2:1 pattern if the Ru atoms were exactly equivalent or a sextet of sextets if they were not. Unfortunately, the high cost and limited availability of isotopically pure ruthenium make definitive work on this matter prohibitive.

Infrared Spectroscopy. Stephenson and Wilkinson[8] reported the far-IR spectrum of $Ru_2(O_2CCH_3)_4Cl$. Bands were observed at 403 and 341 cm^{-1}, which they assigned to Ru–O and Ru–Cl stretching modes, respectively. The latter is where a terminal metal chloride stretch would normally occur. However, in $Ru_2(O_2CR)_4Cl$ the chlorides are bridging with a very long and thus weak Ru–Cl bond. Thus one would expect ν(RuCl) to occur at a much lower frequency. We observed a strong absorption band at 195 cm^{-1} in $Ru_2(but)_4Cl$ (CsI pellet), which we believe to be ν(RuCl). A strong band was also seen at 460 cm^{-1}, which could be the asymmetric ν(RuO) with a_{2u} symmetry in D_{4h}. Medium-intensity bands were also observed at 342 and 375 cm^{-1}. The assignment of these bands is uncertain.

MO Schemes and Theoretical Calculations. The short Ru–Ru distance (2.281 vs. 2.65 Å in Ru metal)[2] implies a strong interaction. Thus, some sort of metal–metal bonding model is needed and various MO schemes have been proposed. In our previous work, our qualitative MO scheme (Figure 1) has been in good agreement with that calculated by Norman et al.[5] Their calculations on the ruthenium system give π^* and δ^* orbitals that are singly occupied and are very close in energy for both $Ru_2(O_2CH)_4^+$ and $Ru_2(O_2CH)_4Cl_2^-$. $Ru_2(but)_4Cl$ is definitely a quartet molecule with the unpaired electrons most likely in π^* and δ^* orbitals. The extensive spin–orbit coupling of these electrons leads to the large zero-field splitting parameter and observation of an EPR spectrum only at low temperatures. Norman et al.[5] have also used their theoretical results on the Ru carboxylate dimer system to calculate EPR parameters for the complex. A shift of $g_\parallel$ by −0.029 from the free-electron value was proposed. This was obtained by considering contributions to $g_\parallel$ from spin–orbit coupling caused by promotion of the unpaired electron in the Ru–Ru δ^* orbital ($2b_{1u}$) to the empty Ru–O σ^* orbital ($4b_{2u}$). This would lead to a shift in $g_\parallel$ of −0.042. Since the originally reported $g_\parallel$ showed a shift of +0.03, Norman et al. also included promotion of electrons from the filled Ru–O σ and π ($3b_{2u}$, $2b_{2u}$) orbitals to δ^* to obtain a g shift of +0.013 leading to a total of −0.029. We observed a $g_\parallel$ shift of −0.056, indicating that only the former mechanism applies and is perhaps underestimated. Qualitatively, a value for $g_\parallel$ slightly less than the free-electron value was predicted resulting from a transition to an empty orbital, and that was in fact observed. A value for $g_\perp$ of 2.18 was predicted, which is quite close to the observed value of 2.200. Many excited states have the proper symmetry to contribute to a shift of $g_\perp$ from the free-electron value. Almost all states arise from transitions to partly filled orbitals, and thus one would

(21) Drago, R. S.; Purcell, K. F. *Prog. Inorg. Chem.* **1964**, *6*, 271.
(22) Cotton, F. A.; Pedersen, E. *Inorg. Chem.* **1975**, *14*, 399.
(23) Cotton, F. A.; Pedersen, E. *J. Am. Chem. Soc.* **1975**, *97*, 303.
(24) Kawamura, T.; Fukumachi, K.; Sowa, T.; Hayashida, S.; Yonezawa, T. *J. Am. Chem. Soc.* **1981**, *103*, 364.
(25) Ginsberg, A. P.; Martin, R. L.; Brookes, R. W.; Sherwood, R. C. *Inorg. Chem.* **1972**, *11*, 2884.

qualitatively predict the positive shift of $g_\perp$ that was observed.

One can also attempt to obtain information from the A values. We observed $A_{iso} = (A_\parallel + 2A_\perp)/3 = 25 \times 10^{-4}$ cm^{-1} and $A_{dip} = (A_\parallel - A_\perp)/3 = -1.67 \times 10^{-4}$ cm^{-1}. Norman et al.[5] have calculated A values by estimating spin polarization at the nucleus and report a value for A_{iso} of 9×10^{-4} cm^{-1}. A dipolar contribution of -0.6×10^{-4} cm^{-1} was also obtained. As these authors point out, these theoretical values are very crude. Ideally, inclusion of a very large number of higher order terms is needed, which would lead to greater electron spin density at the nucleus. The value reported here for $A_\parallel$ (21.7×10^{-4} cm^{-1}) is much different from the previously reported value ($9 (\pm 3) \times 10^{-4}$ cm^{-1}), which causes both A_{iso} and A_{dip} to be in much better agreement with the rough theoretical values.

Conclusions. $Ru_2(but)_4Cl$, a typical example of the ruthenium carboxylate dimer, was studied with use of variable-temperature powder magnetic susceptibility and frozen-solution EPR spectroscopy at 4 K. The complex is an $S = {}^3/_2$ system as was originally proposed.[8] In contrast to earlier suggestions,[4] there are no noticeable interdimer magnetic effects in spite of the polymeric solid-state structure of the complex. The complex does exhibit large zero-field splitting due to spin–orbit coupling. Electron spin density is delocalized over both Ru atoms as with other metal carboxylate dimer radicals. It is possible that the two Ru atoms are not exactly equal, but this difference cannot be resolved without isotopically pure Ru. Far-IR spectroscopy showed a previously unreported ν(RuCl) band. The experimental results provide support for the MO scheme of Norman et al.[5]

Acknowledgment. We thank the National Science Foundation for support of this research. The assistance of Mark Timken with the magnetic susceptibility programs and Jeffrey Cornelius with the EPR programs is gratefully acknowledged.

Registry No. $Ru_2(but)_4Cl$, 53370-31-3.

Contribution from the Departments of Chemistry, University of Florida, Gainesville, Florida 32611, and University of Illinois, Urbana, Illinois 61801

EPR Spectra and Bonding in the 2:1 Base Adducts of $Rh_2(carboxylate)_4^+$

RUSSELL S. DRAGO,* RICHARD COSMANO, and JOSHUA TELSER

Received January 10, 1984

In this paper, EPR studies are reported on a series of 1:1 and 2:1 adducts of $Rh_2(butyrate)_4^+$. The results provide a simplified interpretation of the EPR spectra of the 2:1 adducts. The key feature is the energy of the additional molecular orbital that arises when the donor lone pair is mixed into the 1:1 adduct to form the 2:1 adduct. When the donor lone pair ionization potential is low (C number is large) and the interaction strong, this σ molecular orbital becomes the HOMO and an EPR signal is detected. When the donor ionization potential is high and the interaction weak, the HOMO is π^* and no EPR spectrum is seen. The EPR spectrum of the cation provides no insight into the question of π-stabilization. Clearly, in the CO adducts the π-back-bonding is slight compared to that of most metal carbonyls but it is a significant fraction of the total weak interaction of CO with this acid. The complexes formed when pyridine or *N*-methylimidazole is added in excess to the radical cation do not have axial symmetry.

Introduction

There is considerable interest in metal-cluster chemistry, and the bimetallic carboxylate systems are among the most extensively studied of these. Numerous theoretical, structural, and reactivity studies of rhodium(II) carboxylates[1] have been reported. The nature of the metal–metal interaction in rhodium(II) carboxylates, as well as the electronic structure of their adducts, has been a source of controversy over the years. X-ray crystal structure results[2] and theoretical MO calculations[3] have often led to conflicting conclusions. Clearly, the energy differences of different electronic states are slight, and the results of calculations remain suspect. Different calculational methods give different results,[3] and all fail to account for all known properties For example, ab initio calculations[3d] lead to a HOMO that is σ in nature while an SCF–Xα–SW approach indicates[3c] it is δ^*. In an attempt to solve the problem in an experimental manner, we reported[4] in 1977 an EPR spectrum for the TMPNO adduct of rhodium trifluoroacetate. The results were interpreted in terms of the simplified MO model shown in Figure 1. The appearance of rhodium hyperfine interactions in the spectrum of the radical, as well as a sizable shift in the g value compared to that of the noncomplexed base, was taken as evidence that some type of π-interaction was occurring between the rhodium atom and the nitroxide radical base.

Calorimetric studies of rhodium(II) butyrate later showed[5] that there was a bonding interaction occurring between the metals and certain axial bases that could not be accounted for by a σ-only bond as viewed in the E and C model. Comparison of the enthalpies of adduct formation with the observed changes in the visible spectrum and the electrochemical behavior of the 1:1 adducts were consistent with the interpretation that the anomalous bonding interaction involved a back-donation of π^*-electron density from high-energy, rho-

* To whom correspondence should be addressed at the University of Florida.

(1) (a) Boyar, E. D.; Robinson, S. D. *Coord. Chem. Rev.* **1983**, *50*, 109 and references therein. (b) Cotton, F. A.; Walton, R. A. "Multiple Bonds Between Metal Atoms"; Wiley-Interscience: New York, 1982; and references therein. (c) Felthouse, T. R. *Prog. Inorg. Chem.* **1982**, *29*, 73 and references therein.

(2) (a) Christoph, G. G.; Halpern, J.; Khare, G. P.; Koh, Y. B.; Romanowski, C. *Inorg. Chem.* **1981**, *20*, 3029 and references therein. (b) Caulton, K. G.; Cotton, F. A. *J. Am. Chem. Soc.* **1971**, *93*, 1914 and references therein. (c) Bursten, B. E.; Cotton, F. A. *Inorg. Chem.* **1981**, *20*, 3042.

(3) (a) Dubicki, K.; Martin, R. L. *Inorg. Chem.* **1970**, *9*, 673. (b) Norman, J. G.; Kolari, H. J. *J. Am. Chem. Soc.* **1978**, *100*, 791. (c) Norman, J. G.; Renzoni, G. E.; Case, D. A. *J. Am. Chem. Soc.* **1979**, *101*, 5256. (d) Nakatsuji, H.; Onishi, Y.; Ushio, J.; Yonezawa, T. *Inorg. Chem.* **1983**, *22*, 1623.

(4) Richman, R. M.; Kuechler, T. C.; Tanner, S. P.; Drago, R. S. *J. Am. Chem. Soc.* **1977**, *99*, 1055.

(5) (a) Drago, R. S.; Tanner, S. P.; Richman, R. M.; Long, J. R. *J. Am. Chem. Soc.* **1979**, *101*, 2897. (b) Drago, R. S.; Long, J. R.; Cosmano, R. *Inorg. Chem.* **1981**, *20*, 2920. (c) Drago, R. S. *Inorg. Chem.* **1982**, *21*, 1697.

0020-1669/84/1323-3120$01.50/0